Chapter 12

Amplitude and Flux Calibration

Anne Dutrey[1,2]

Anne.Dutrey@obs.ujf-grenoble.fr

[1] IRAM, 300 rue de la Piscine, F-38406 Saint Martin d'Hères, France

[2] LAOG, BP53, F-38041 Grenoble Cedex 9, France

Calibration compensates for imperfections and unknowns in the instrument use, including antenna defects (surface quality, focus), pointing errors, atmospheric transmission and fluctuations, receiver and backend gain and instabilities, etc...All of them are varying in time. In addition, calibrated data are also expressed in a reliable physical unit.

This lecture is then cut in three parts, of equal importance:

1. The single-dish calibration of the amplitude: its errors and biases
2. The flux density calibration which gives the absolute scale of the data
3. The temporal amplitude calibration of interferometric data

12.1 Definition and Formalism

From Lucas lecture (Chapter 9), Eq. 9.1, the baseline-based observed visibility $\widetilde{V}_{ij}(t)$ is linked to the true visibility V_{ij} of the source by:

$$\widetilde{V}_{ij}(t) = \mathcal{G}_{ij} V_{ij} + \epsilon_{ij}(t) + \eta_{ij}(t) \tag{12.1}$$

In antenna-based calibration, $\mathcal{G}_{ij}$ can also be written as:

$$\mathcal{G}_{ij} = g_i(t) g_j^*(t) = a_i(t) a_j(t) e^{i(\phi_i(t) - \phi_j(t))} \tag{12.2}$$

Hence, for antenna i, the antenna-based amplitude correction for the lower sideband a_i^L is given by

$$a_i^L(t) = T_{cal_i}^L(t) G_i^L(\nu, t) \Gamma_i(t) \tag{12.3}$$

and for the upper sideband:

$$a_i^U(t) = T_{cal_i}^U(t) G_i^U(\nu, t) \Gamma_i(t) \tag{12.4}$$

where $T_{cal_i}^U$ and $T_{cal_i}^L$ are the corrections for the atmospheric absorption (see Chapter 10), in the upper and lower sidebands respectively. Γ_i the antenna gain (affected by pointing errors, defocusing, surface status and systematic elevation effects). Note that Eqs.12.3-12.4 do not include the decorrelation factor f (see Chapter 9 by R.Lucas) because this parameter is baseline-based. We assume here decorrelation is small enough, i.e. $f = 1$; if not, a baseline-based amplitude calibration may be required.

$G_i^L(\nu, t)$ and $G_i^U(\nu, t)$ are the electronics gains (IF chain+receiver) in the lower and upper sidebands, respectively. The receiver sideband gain ratio is defined as $G_i^{UL}(\nu, t) = G_i^U(\nu, t)/G_i^L(\nu, t)$. The sideband gain ratio is to first order independent of the frequency ν within the IF bandwidth. The derivation of the receiver gains is given in Chapter 9. At Bure, the receivers and the IF chain are very stable and these values are constant with time (and equal to G_i^{UL}, G_i^U and G_i^L, respectively, since we also neglected their frequency dependence within the IF bandwidth). They are measured at the beginning of each project on a strong astronomical source. Moreover in Eq.12.3-12.4, we use the fact that for a given tuning, only the receiver gains and the atmospheric absorption have a significant dependence as a function of frequency.

Section 12.2 will focus on the corrections for the atmospheric absorption ($T_{cal_i}^U(t)$,$T_{cal_i}^L(t)$) and the possible biases they can introduce in the amplitude.

In the equations above, the amplitudes can be expressed either in Kelvin (antenna temperature scale, T_A^*, $\eta_f = \eta_b$) or in Jy (flux density unit, 1 Jy= 10^{-26} W m^{-2}Hz^{-1}). The derivation of the conversion factor between Jy and K, in Jy/K, $\mathcal{J}_{iS}$ (single-dish mode) and $\mathcal{J}_{iI}$ (interferometric mode) and its biases will be detailed in section 12.3 which is devoted to the flux density calibration.

Finally Section 12.4 will deal with the understanding of the terms $\Gamma_i(t)$ and f, the amplitude calibration of interferometric data.

12.2 Single-dish Calibration of the Amplitude

The goal of this part of the calibration is to measure the atmospheric transparency above each antenna.

This calibration is done automatically and in *real-time* but it can be redone *a posteriori* if one or several parameters are wrong using the CLIC command `ATMOSPHERE`. However, for 99 % of the projects, the single-dish calibration is correct. Moreover, we will see in this section that in most cases, even with erroneous calibration parameters, it is almost impossible to do an error larger than $\sim 5\%$.

For details about the properties of the atmosphere, the reader has to refer to Chapter 11 while the transmission of the atmosphere at mm wavelengths is described in Chapter 10. Most of this lecture is extracted from the documentation "Amplitude Calibration" by [Guilloteau 1990] for single-dish telescope and from [Guilloteau et al. 1993].

Since all this part of the calibration is purely antenna dependent and in order to simplify the equations, the subscript $_i$ will be systematically ignored. In the same spirit, the equations will be expressed in T_A^* scale taking $\eta_f = \eta_b$ (see [Guilloteau 1990]).

The atmospheric absorption (*e.g.* for the lower side-band T_{cal}^L) can be expressed by

$$T_{cal}^L = \frac{(T_{load}(1 + G^{UL}) - T_{emi}^L - G^{UL} T_{emi}^U)}{\eta_f e^{-\tau^L / \sin(Elevation)}} \tag{12.5}$$

where T_{load} is the hot load and T_{emi}^L and T_{emi}^U are the noise temperature received from the sky in the lower an upper sidebands respectively (for the IRAM interferometer, the difference in frequency between the upper and lower sidebands is ~ 3 GHz).

The system temperature T_{sys} is given by:

$$T_{sys}^L = T_{cal}^L \times \frac{M_{atm}}{M_{load} - M_{cold}} \tag{12.6}$$

The main goal of the single-dish calibration is to measure T_{cal} (hence T_{sys}) as accurately as possible.

At Bure, during a standard atmospheric calibration, the measured quantities are:

- Phase 1, M_{atm}: the power received from the sky
- Phase 2, M_{load}: the power received from the hot load
- (Phase 3), M_{cold}: the power received from the cold load

T_{rec}, the noise temperature of the receiver, is deduced from the measurements on the hot and cold loads at the beginning of each project and regularly checked. The phase 2 (hot load) is also not systematically done (this remains valid because temperature drifts on the hot load are on timescales of several hours). The receiver sideband ratio G^{UL} is also measured at the beginning of each project (see Chapter 9). T_{emi}, the effective temperature seen by the antenna, is given by

$$T_{emi} = \frac{(T_{load} + T_{rec}) \times M_{atm}}{M_{load}} - T_{rec} \tag{12.7}$$

Moreover, T_{emi} which is measured on the bandwidth of the receiver, can be expressed as the sum of T^L_{emi} and T^U_{emi} (a similar expression exists for T_{sky}):

$$T_{emi} = \frac{T^L_{emi} + T^U_{emi} \times G^{UL}}{1 + G^{UL}} \tag{12.8}$$

T_{emi} is directly linked to the sky temperature emissivity (or brightness temperature) T_{sky} by:

$$T_{sky} = \frac{T_{emi} - (1 - \eta_f) \times T_{cab}}{\eta_f} \tag{12.9}$$

were T_{cab} is the physical temperature inside the cabin and η_f, the forward efficiency, which are both known (or measurable) quantities.

Our calibration system provides then a direct measurement of T_{emi} and hence of T_{sky}, which is deduced from quantities accurately measured. Hence, in Eq.12.5 the only unknown parameter remains τ^L, the opacity of the atmosphere at zenith, which is iteratively computed together with T_{atm} the physical atmospheric temperature of the absorbing layers. This calculation is performed by the atmospheric transmission model ATM (see Chapter 10) and the documentation "Amplitude Calibration").

The opacity τ^L (or more generally τ_ν) comes from two terms:

$$\tau_\nu = A_\nu + B_\nu \times w \tag{12.10}$$

A_ν and B_ν are the respective contributions to O_2 and H_2O, the water vapor content w is then adjusted with T_{atm} by the model ATM to match the measured T_{sky}. The ATM model works as long as the hypothesis done on the structure of the atmosphere in plane-parallel layers is justified, as it is usually the case for standard weather conditions.

12.2.1 Low opacity approximation and implication for T_{cal}

When the opacity of the atmosphere is weak ($\tau_\nu < 0.2$) and equal in both image and signal bands, T_{cal} is mostly dependent of T_{atm} and both of them can be considered as independent of τ_ν and hence w.

In the conditions mentioned above, τ_ν can be eliminated from Eq.12.5. The equation becomes:

$$T^L_{cal} = \frac{\eta_f \times (1 + G^{UL}) \times T_{atm}}{\eta_b \times (1 - \eta_f \times \frac{T_{cab} - T_{atm}}{T_{cab} - T^L_{emi}})} = \frac{(1 + G^{UL}) \times T_{atm}}{(1 - \eta_f \times \frac{T_{cab} - T_{atm}}{T_{cab} - T^L_{emi}})} \tag{12.11}$$

(details about the derivation of Eq.12.11 are given in the documentation "Amplitude Calibration" by S.Guilloteau). In Eq.12.11, the unknown is T_{atm}, the physical temperature of the absorbing layers. T_{atm} is mostly dependent on the outside temperature, pressure and site altitude and weakly on τ_ν. For this reason, T_{cal} and T_{sys} remain correct even if w and hence τ_ν are not properly constrained.

Item	T_{cab}	T_{rec}	η_f
Typical Error	2 K	10 K	0.01
Induced variation (in %)	0.7	0.3	1.3

Table 12.1: Percentage error on amplitude scale introduced by erroneous input parameters.

Figures 12.1 and 12.2 illustrate this point. Thick lines correspond to the exact equation (Eq.12.5) and dashed lines to the approximation (Eq.12.11). The comparison between Eq.12.11 and 12.5 was done for three common cases 1) at 87 GHz, with $G^{UL} = 10^{-2}$, 2) at 115 GHz, with $G^{LU} = 0.5$ and at 230 GHz, with $G^{UL} = 0.5$. For the 15-m dishes, the forward efficiencies used are $\eta_f = 0.93$ at 3 mm and $\eta_f = 0.89$ at 1.3 mm. Fig.12.1 is done for a source at $elevation = 20^0$ and Fig.12.2 for a source at $elevation = 60^o$.

The following points can be deduced from these figures:

1. As long as $T^L_{sky} = T^U_{sky}$, the equation 12.11 remains valid even at high frequencies > 200 GHz and for $w > 5$ mm.
2. This comes from the fact the T_{atm} is mostly independent of the atmospheric water vapor content.
3. As soon as $T^L_{sky} \neq T^U_{sky}$, the equation 12.11 is not valid. Note also that the error is about constant with the opacity because T_{atm} is mostly independent of the atmospheric water vapor content. Moreover at 115 GHz, the atmospheric opacity is dominated by the 118 GHz Oxygen line and cannot be below 0.2 and the amount of opacity added by the water vapor is small. T_{cal} remains mostly constant with w.

At mm wavelengths, the derivation of the T_{cal} (or T_{sys}) using an atmospheric model is then **quite safe**.

12.2.2 Absolute errors on T_{cal} due to instrumental parameters

The equations above show that T_{cal} is also dependent of the instrumental parameters T_{rec}, η_f and T_{load}. These parameters can also lead to errors on T_{cal}. Derivatives of the appropriate equations are given in the IRAM report "Amplitude Calibration". Applying these equations and taking $T_{atm} = 240$ K, $T_{load} = 290$ K and $T_{emi} = 50$ K, the possible resulting errors are given in the table 12.1.

As a consequence, the most critical parameter of the calibration is the Forward Efficiency η_f. This parameter is a function of frequency, because of optics surface accuracy, but also of the receiver illumination. If η_f is underestimated, T_{sky} is underestimated and you may obtain anomalously low water vapor content, and vice-versa.

The sideband gain ratio G^{UL} is also a critical parameter. G^{UL} is not only a scaling factor (see Eq.12.5), but is also involved in the derivation of the atmospheric model since the contributions from the atmosphere in image and signal bands are considered. This effect is important only if the opacities in both bands are significantly different, as for the J=1-0 line of CO.

Eq.12.5 shows that as soon as the receivers are tuned in single side band ($G^{UL} < 10^{-2}$ or rejection > 20dB), the effect on T^L_{cal} is insignificant. Errors can be significant when the tuning is double-side band with values of G^{UL} around $\sim 0.8 - 0.2$. For example, when the emissivity of the sky is the same in both bands ($T^U_{sky} = T^L_{sky}$), the derivative of Eq.12.8 shows that an error of 0.1 on $G^{UL} = 0.5$ leads to $\frac{\Delta T_{cal}}{T_{cal}} \simeq \frac{dG^{UL}}{1+G^{UL}} \sim 6.5\%$.

However, this problem is only relevant to single-dish observations and should not happen in interferometry because as soon as three antennas are working, G^{UL} can be accurately measured (see Chapter 9). At Bure the accuracy on G^{UL} is better than about 1 % and the system is stable on scale of several hours.

12.2.3 Relative errors or errors on T^L_{cal}/T^U_{cal}

Following Eq.12.5, the side band ratio will be affected by the following term:

$$T = \frac{e^{(\Delta(\tau^L - \tau^U))}}{\sin(Elevation)} \tag{12.12}$$

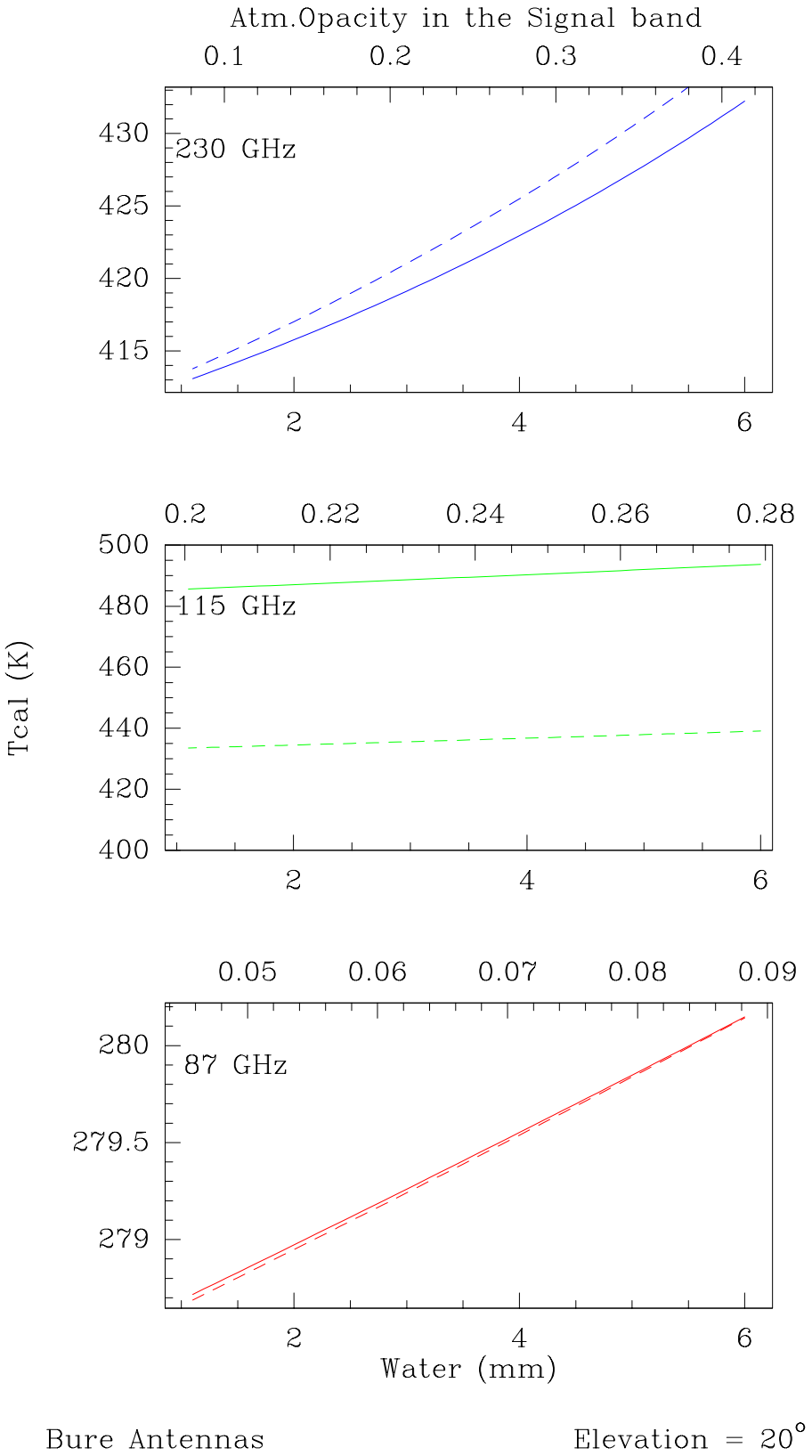

Figure 12.1: Calibration temperature as function of water vapor (or opacity) at 87, 115 and 230 GHz for a source at 20 degrees elevation. Parameters are taken for the Bure interferometer (see text). Thick lines correspond to the exact equation (Eq.12.5) and dashed lines to the approximation (Eq.12.11).

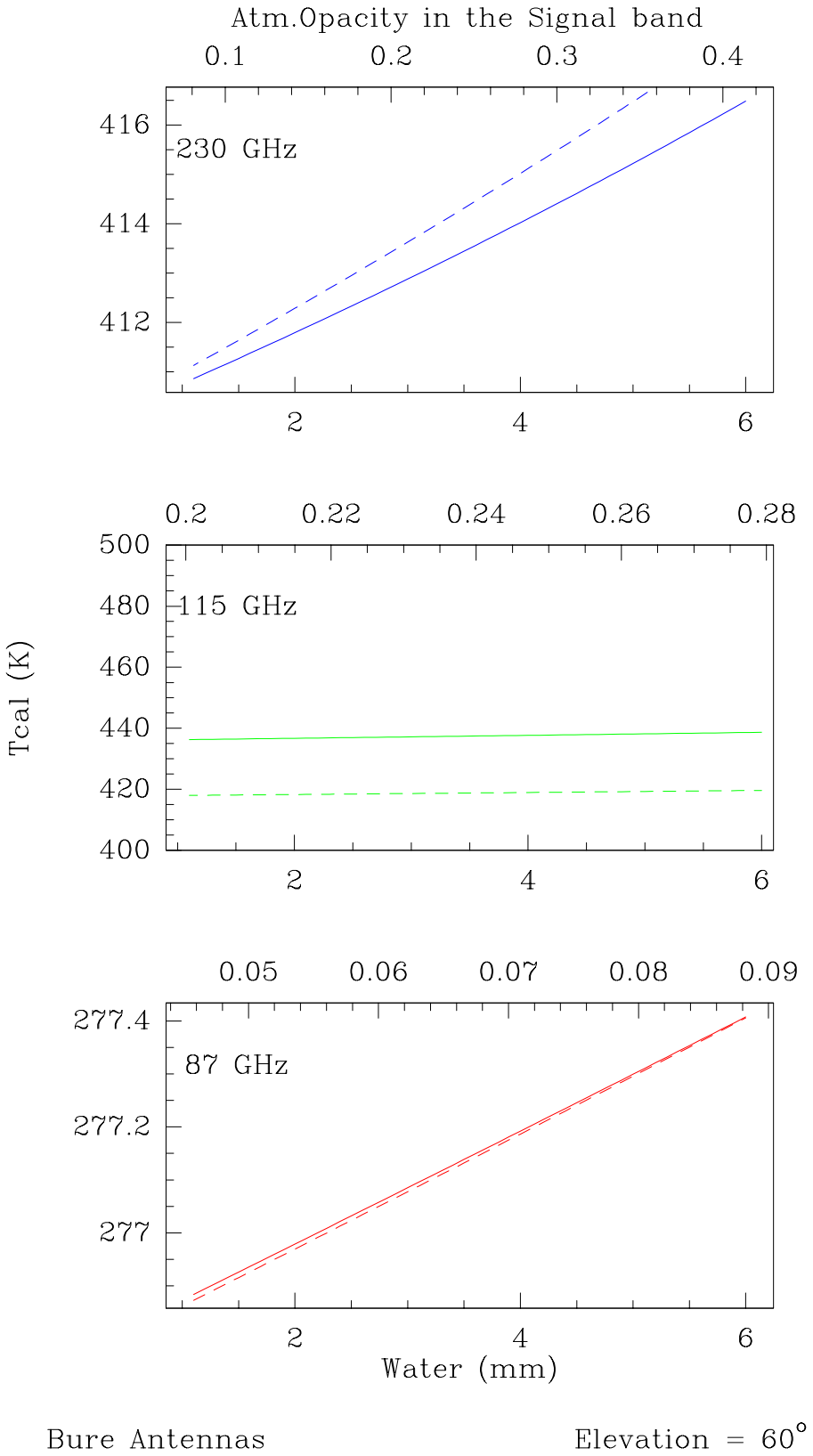

Figure 12.2: Calibration temperature as function of water vapor (or opacity) at 87, 115 and 230 GHz for a source at 60 degrees elevation. Parameters are taken for the Bure interferometer (see text). Thick lines correspond to the exact equation (Eq.12.5) and dashed lines to the approximation (Eq.12.11).

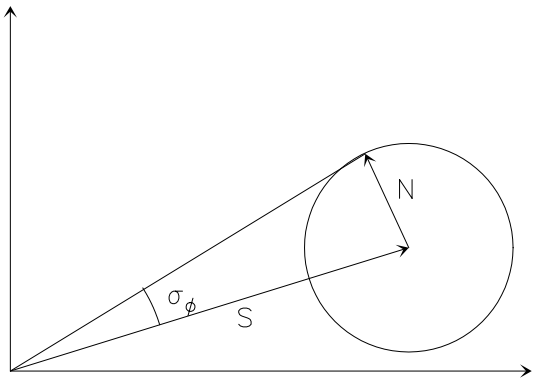

Figure 12.3: Phase error resulting from limited S/N ratio. $\sigma_\phi \approx 1/(S/N)$.

where $\Delta(\tau^L - \tau^U)$ is the error on the sideband zenith opacity difference. This difference is maximum at frequencies corresponding to a wing of an atmospheric line, for example when observing around 115 GHz, near the O_2 line at 118 GHz. As example, taking the frequencies of 112 and 115 GHz for a source at 20^o in elevation and a zenith opacity difference $(\tau^L - \tau^U) = 0.150$, an error of 0.030 on this difference (coming from A_ν) will give an error of less than 1% on the gain G^{UL}. Moreover errors on Oxygen lines are very unlikely because the content in Oxygen in the atmosphere is relatively well known and only varying with the altitude of the site.

At the same frequencies, an error of 5 mm (which would be enormous) on the water vapor content will only induce an error of 1% on the gain. Around such low frequency and for small frequency offsets, the water absorption is essentially achromatic. Improper calibration of the water vapor fluctuations will then result in even smaller errors since this is a random effect.

12.2.4 Estimate of the thermal noise

The resulting thermal noise is given by

$$1\sigma = \frac{2kT_{sys}}{\eta A\sqrt{\Delta\nu \times t}}(\mathrm{K}) \tag{12.13}$$

where k is the Boltzmann's constant, A is the geometric collecting area of the telescope, η the global efficiency factor (including decorrelation, quantization, etc...), $\Delta\nu$ the bandwidth in use and t the integration time. The resulting error on the phase determination is inversely proportional to the signal to noise ratio, as shown in Fig.12.3.

12.3 Flux Calibration (visitor's nightmare)

More details are found in the documentation "Flux measurement with the IRAM Plateau de Bure Interferometer"[1] by A.Dutrey & S.Guilloteau.

12.3.1 Introduction

Because of the focus and pointing errors, and possible drifts in receiver gains, amplitude calibration has always been difficult at mm wavelengths. In addition to these basic single-dish effects, the variable amount of decorrelation introduced by phase noise (atmospheric and/or instrumental) make it difficult, if not impossible, for an interferometer to measure absolute flux densities.

All measurements need to be relative to some source of known flux. In practice, planets are used because they are among the few astronomical objects sufficiently strong at millimeter wavelengths for which flux density predictions are possible and sufficiently accurate. They are then used as primary calibrators to

[1] http://iram.fr/PDBI/flux/flux.html

Antenna number	3 mm efficiency (Jy/K)	1.3 mm efficiency (Jy/K)
1	22	37
2	21	27
3	21	36
4	21	29
5	22	34

Table 12.2: Conversion factor from K to Jy for the 15-m antennas of Plateau de Bure

bootstrap the flux of the stronger quasars which are point sources. Since the quasars are highly variable, a regular monitoring (each month) is needed. These observations require a very good weather with a small amount of precipitable water vapor (< 4 mm) and a stable atmospheric phase. If not properly taken into account, the quasar variability can produce an error in the flux scale during one configuration which does not result in a simple scale factor in the final image, but introduces artifacts.

12.3.2 Calibration procedure at Bure

Some basic points Because of the physics of quasars, the spectral index may be variable with time as the source intensity. Simultaneous measurements at 2 frequencies are thus needed to estimate it accurately, IRAM instruments (30-m and PdBI) use the frequencies of 86.7 GHz and 228 GHz. At the 30-m, flux density measurements are done during the pointing sessions while they are performed in special sessions at Bure, usually after baseline measurements.

The results of the flux sessions are regularly reduced and published in an internal report (usually each 4 months). These reports are currently available on the web, in the local IRAM page (see[2]).

How we proceed at Bure In practice, it is impossible (and not necessary) to follow all the quasars used as amplitude calibrator at the IRAM interferometer. Monitoring of the RF bandpass calibrators which are strong quasars with flux density > 2 Jy (no more than 4-8 sources) is enough. In the meantime, planets are observed as primary calibrators. These sessions require to calibrate the atmosphere (T_{sys}) on each source and to check regularly the focus.

At the Bure interferometer, the flux density measurements on quasars are done by pointings in interferometric mode. Pointings on planets are actually done in total power mode because they are resolved by interferometry and strong enough. Total power intensity is not affected by the possible decorrelation due to atmospheric phase noise. However, it is then necessary to accurately determine the efficiencies of the individual antennas (conversion factor in Jy/K) in interferometric mode ($\mathcal{J}_I$) and in single-dish mode ($\mathcal{J}_S$).

Determining the antenna efficiencies (Jy/K) For each flux session, $\mathcal{J}_S$ is measured on planets by comparison with the models (see GILDAS programs ASTRO or FLUX).

For a given antenna, the interferometric efficiency $\mathcal{J}_I$ is always $\geq \mathcal{J}_S$. Pointing measurements in interferometric mode are not limited by the atmospheric decorrelation because the timescale of the atmospheric decorrelation is usually significantly larger than the time duration of the basic pointing integration time ($<$ a few sec). On the contrary, all instrumental phase noise on very short timescale can introduce a significant decorrelation and degrades $\mathcal{J}_I$. This is what may happen from time to time at a peculiar frequency due to a bad optimization of the receiver tuning.

For example, in the initial 1.3 mm observations, strong decorrelation was introduced by the harmonic mixer of the local oscillator system which degraded $\mathcal{J}_I$ by a factor of $2-4$ depending of the antennas. This problem has been solved recently. Now at 3 mm, it is reasonable to neglect the instrumental noises and take $\mathcal{J}_I = \mathcal{J}_S$. At 1.3 mm, the new harmonic mixers have been installed only recently and statistics on the site are rare but laboratory measurements show that the loss in efficiency should be small. The Table 12.2 gives the antenna efficiencies $\mathcal{J}_S$, as measured in flux sessions or by holography. These values

[2]http://iram.fr/LI/astro.html

are the current efficiencies (as of November 1997); older values are given in flux reports. They assume that the focus is optimum and do not include any instrumental phase noise. $\mathcal{J}_I$ agrees usually within 10 % at 3 mm and 15 % at 1.3 mm with $\mathcal{J}_S$, note that $\mathcal{J}_I$ must be $\geq \mathcal{J}_S$.

Being able to cancel out most of the instrumental phase noise even at 1.3 mm makes the IRAM interferometer a very reliable instrument. It is reasonable to think that, in the near future, the flux calibration will be systematically performed at Bure at the beginning of each project by reference to the antenna efficiencies. This is indeed already the case: after pointing and focusing, we systematically measure the flux of calibrators when starting a new project (data labeled `FLUX` in files). Up to now, for typical weather conditions, most (more than 90 %) of the flux measured at 3 mm are correct within 10 % and more than 60 % at 1.3 mm are within 15 %.

CRL 618 and MWC 349 as secondary flux calibrators Finally, for each project, a complementary flux check is systematically done using the continuum sources CRL 618 or MWC 349 (pointing + cross-correlations). However these sources must be used with some caution. CRL 618 is partially resolved in A and B configurations at 3 mm and in A,B,C at 1.3 mm. Moreover it has strong spectral lines which may dominate the average continuum flux; this must be checked before using it for flux estimates. MWC 349 is unresolved and remains a reliable reference in all antenna configurations. The only strong lines for MWC 349 are the Hydrogen recombination lines. The adopted flux densities are:

For CRL618 (see flux reports 13 and 15):

- CRL618 F(87 GHz) = 1.55 Jy (+/ − 0.15)
  At 87 GHz, the flux density of CRL 618 (free-free emission from the HII region) has increased since 1990 (where it was $\sim$ 1.1 Jy instead of 1.55 Jy).

- CRL618 F(231.9 GHz) = 2.0 Jy (+/ − 0.3),
  from [Martin-Pintado et al. 1988]. Since the flux density has increased at 87 GHz, this value needs to be observationally confirmed. Beware of the line contamination which can be high in CRL618.

For MWC349:

- Spectrum of MWC349 F(ν) = 1.69(ν/227 GHz)$^{0.6}$

- MWC349 F(87 GHz) = 0.95 Jy

- MWC349 F(227 GHz) = 1.69 Jy

These values agree within 1 σ with the measurement performed at 87 GHz [Altenoff et al. 1994], (0.87 $\pm$0.09 Jy).

12.3.3 Determining the absolute flux scale on a project

The method Fig.12.4 is a printout of the "standard calibration procedure" used in CLIC. This procedure uses the CLIC command `SOLVE FLUX` which works on cross-correlation only as follows:

1. The flux of the reference source is fixed to F(Ref)

2. F(Ref) is used to measure the antenna efficiency by dividing it by antenna temperature of the reference (T_A^*(Ref)): $\mathcal{J}_I = F(\text{Ref})/T_A^*(\text{Ref})$

3. $\mathcal{J}_I$ is used to compute the flux of all other sources in the index: $F(source) = \mathcal{J}_I \times T_A^*(source)$

The flux density of the amplitude calibrators will be used in the final step of the amplitude calibration to fix the flux of the source of astronomical interest.

The practice In the automatic procedure, the reference sources are the calibrators where **Fixed flux** is set to **YES** and the reference values are in the variable **Input Flux**. **Flux in file** corresponds to the value stored with the data (by using the observational command `FLUX`, see Chapter 8 for details). The calculation is performed by clicking on `SOLVE` and the results are displayed inside the variable **Solved Flux**.

If you want to iterate using one of these values as reference, you need to write it in the variable **Input Flux** and set **Fixed flux** to **YES**. Like in the CLIC command `SOLVE FLUX`, the individual antenna efficiencies ($\mathcal{J}_I$) are computed; these values are only averaged values on the time interval using all sources. They are then affected by many small biases like pointing or focus errors and atmospheric decorrelation and they are usually worse than the canonical values given in table 12.2 (for biases, see end of this section).

When you are satisfied by the flux calibration, you need to click on the following sequence of buttons: 1) `Get Results` in order to update the internal variables of the CLIC procedure, 2) `Store` to save the flux values inside the header file (`hpb` file) and 3) `Plot` to display the result of your calibration. The plot shows the inverse of the antenna efficiencies ($1/\mathcal{J}_I$) versus time for all selected sources. If the flux calibration is correct, all sources must have the same value *e.g.* $1/\mathcal{J}_I$. This plot is systematically done in mode `amplitude scaled` (written on the top left corner). In this mode, the antenna temperature of each source $T_A^*(source)$ in K is divided by its assumed (variable **Input flux**) flux density $F(source)$ in Jy (the value you have just stored), the result is then $T_A^*(source)/F(source) = 1/\mathcal{J}_I(source)$ which must be the same for all sources and equal to $1/\mathcal{J}_I$. If it is not the case, for example if one source appears systematically lower or higher than the others, this means that its flux is wrong and you need to iterate.

Note that the scan range, applied on all calibrators, which is by default the scan range of the "standard calibration procedure" can be changed. This option is useful when there is some shadowing on one calibrator because the shadowing can strongly affect the result of a `SOLVE FLUX`. If you change the scan range, do not forget to click on `UPDATE`.

12.3.4 Possible biases and remedies

Flux densities are more important than efficiencies In the final amplitude calibration performed on the source (see next section), the flux of the source is determined by reference to the flux of the amplitude calibrator which is usually also the phase calibrator. This means that the averaged efficiencies $\mathcal{J}_I$ computed by `SOLVE FLUX` and the automatic procedure are not directly used and in many case variations of $\mathcal{J}_I$ does not affect the accuracy of the final amplitude calibration because they are corrected. It is then fundamental to have a good estimate of the flux of the amplitude calibrator but not necessarily to know precisely the averaged $\mathcal{J}_I$.

Possible biases Using the automatic procedure, the following biases may occur:

1. There is some shadowing on the reference source. The estimate of the $\mathcal{J}_I$ can then be wrong: use another reference.

2. One or several antennas are off focus: $\mathcal{J}_I$ is larger than $\mathcal{J}_S$ but flux densities can still be correct if there is no significant focus drift during the time interval used to measure the fluxes. If the data are affected by a significant focus drift, this also affects the accuracy of the flux measurements. Depending of the observation time of the reference and of the sources, the estimated flux densities can be either too low (reference taken at the beginning when the focus is correct, sources at the end when the focus is off) or too high (opposite situation). In both cases, it is necessary to check the focus (or have a look at the `show.ps` file). If no drift occurs, the measured fluxes are correct. If a drift occurs, the flux calibration must be done on a smaller interval of time where the focus drift remains negligible.

3. The pointing on the reference is bad. $\mathcal{J}_I$ is then overestimated implying that the flux of all other sources (with good pointing) is also overestimated. Check the pointing on the possible reference sources (or see the `show.ps` file) and select a better reference.

4. There is a strong atmospheric decorrelation because flux measurements are performed on cross-correlations of about 4 minutes when the atmospheric phase fluctuations are high (check them on

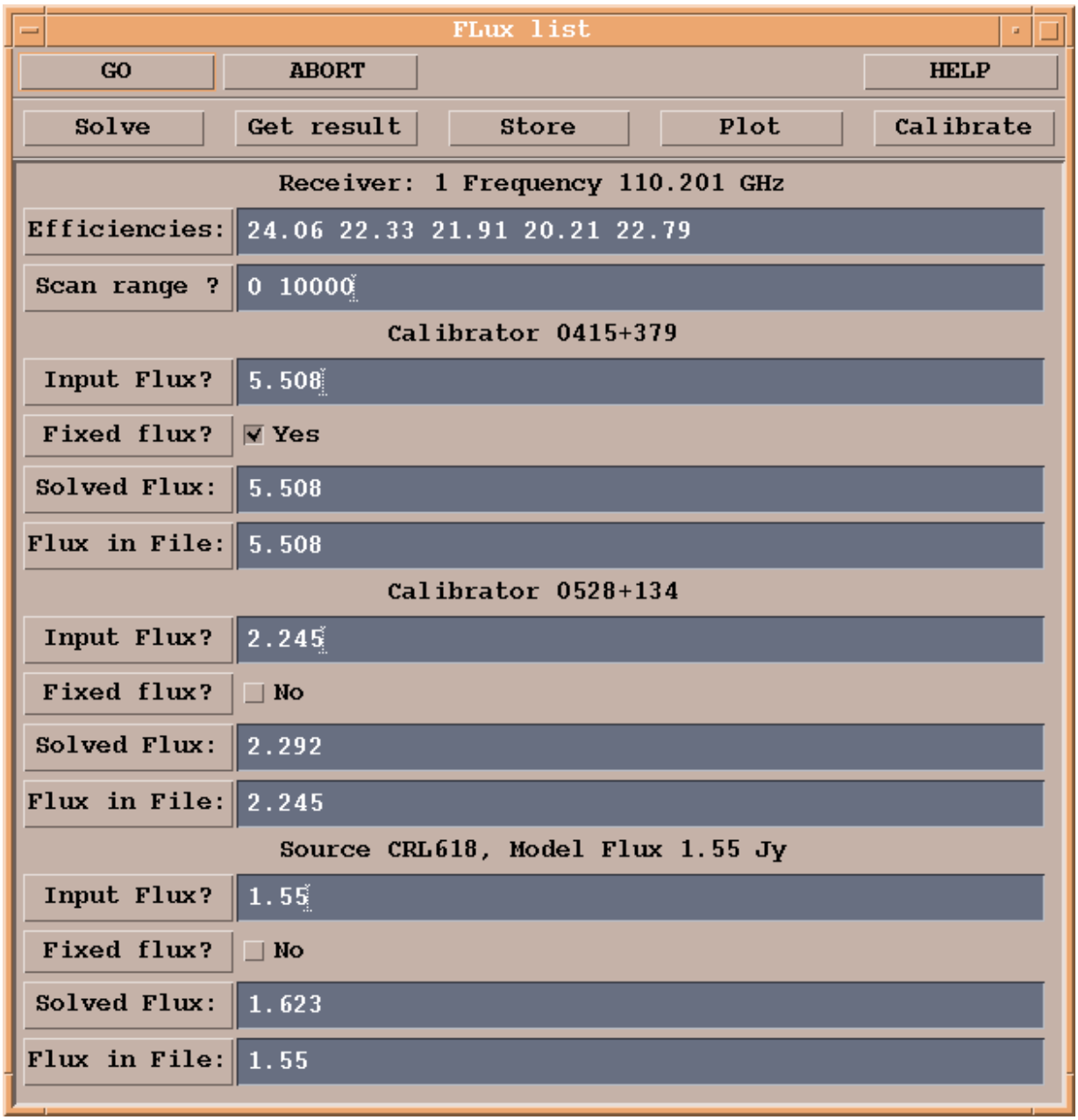

Figure 12.4: User interface of the "standard calibration procedure" of CLIC corresponding to the flux calibration.

an individual cross-correlation taken on a strong quasar *e.g.* the RF calibrator). There are two possibilities: i) when the atmospheric correction works well (as it is usually the case), just apply it to measure the fluxes; ii) if not, the data may be usable at 3 mm by selecting the best scans on a small interval of time but at 1.3 mm data are useless.

5. The interferometric efficiencies $\mathcal{J}_I$ are really very different to $\mathcal{J}_S$ because there is a wonderful mixing of the points mentioned above... Ask to an expert (e.g. your local contact...).

Note that the biases 3) and 4) do not affect flux estimates when they are performed on pointing data (as in sessions of flux measurements).

12.3.5 The program FLUX

This program is not used by the external users of the PdBI but IRAM astronomers to provide reliable flux density of quasars to visitors (see flux reports). A description of the program is given in "Flux measurement with the IRAM Plateau de Bure Interferometer"[3] by A.Dutrey & S.Guilloteau

12.4 Interferometric Calibration of the Amplitude

For antenna i, the antenna-based amplitude correction is given by (Eq.12.3 and 12.4).

$$a_i^K(t) = T_{cal_i}^K(t) G_i^K(\nu, t) \Gamma_i(t) \tag{12.14}$$

where K = U or L. The decorrelation factor f (see Chapter 9) is not taken into account here because it is fundamentally a baseline-based parameter.

In a baseline-based decomposition, the complex gain of baseline ij, $\mathcal{G}_{ij}$ is given by:

$$\mathcal{G}_{ij}^K(t) = f \times a_i(t) a_j(t) e^{i(\phi_i(t) - \phi_j(t))} \tag{12.15}$$

and the amplitude of the baseline ij is $\mathcal{A}_{ij}$

$$\mathcal{A}_{ij}^K(t) = f \sqrt{T_{cal_i}^K T_{cal_j}^K(t) G_i^K(\nu, t) G_j^K(\nu, t) \Gamma_i(t) \Gamma_j(t)} \tag{12.16}$$

We will discuss first the term Γ_i and estimate then the decorrelation factor f, before giving a global scheme of the amplitude calibration.

12.4.1 Correction for the antenna gain $\Gamma_i(t)$

The antenna gain $\Gamma_i(t)$ corresponds to losses due to the antenna, mainly focus (F_i) and pointing (P_i) errors coming from thermal variations of the antenna structure and surface.

$$\Gamma_i(t) = P_i(t) \times F_i(t) \tag{12.17}$$

At Bure, we now check and correct automatically the pointing and the focus each hour. This correction is then done mainly in real time. This has improved a lot the quality of the data at 1.3 mm. However, it is necessary in some cases to add a break in the amplitude (but not in the phase) fitting in order to take into account a focus error or a loss of amplitude due to pointing errors.

Note that an error on the focus of 0.1 mm at 1.3 mm will introduce a phase error of $\frac{4\pi}{\lambda} \times \frac{180}{\pi} \times 0.1 \sim 55^o$ and a loss in amplitude of $\sim 3 - 5\%$.

[3] http://iram.fr/PDBI/flux/flux.html

Atmospheric Timescales	Amplitude coherence	Phase correction	Comments
$\Delta t \geq 1-2$ hours	No loss	Corrected by temporal phase fitting	Large scales are corrected
1 min$\leq \Delta t \leq 1-2$ hours 1 min = scan duration	No correction can be partially corrected	rms ($=\Delta\phi$) of temporal phase fit $f = e^{(-\Delta\phi^2/2)}$ **Radio Seeing**	**Loss of flux** *a-posteriori* correction by comparison with some reference sources: images of calibrators of known flux
$\Delta t \leq 1$ min	Usually corrected Radiometric phase correction	"MONITOR 0" $\equiv$ mean value of the phase in 1 min	works usually well except for bad weather conditions

Table 12.3: Useful decomposition of the atmospheric phase fluctuations above the Plateau de Bure interferometer. This qualitative scheme is done to show which timescales are corrected by the calibration of the Bure data and the radiometric phase correction working at Bure.

12.4.2 Estimate of the atmospheric decorrelation factor f

Details about the origin of f are given in Chapter 11. I will discuss here the practical implementation of the atmospheric phase correction done in real-time and in CLIC. More details are given in the IRAM report "Practical implementation of the atmospheric phase correction for the PdBI" by R.Lucas.

The atmospheric phase fluctuations are due to different time varying water vapor content in the line-of-sight of each antenna through the atmosphere. Between antennas i and j, this introduces a decorrelation factor $f \sim e^{-\Delta\phi_{ij}^2/2}$ on the visibility V_{ij}. This term, non-linear, cannot be factorized by antenna. Moreover due to the physical properties of the atmosphere, there are several timescales. One can correct partially some, but not all, of them.

At Bure the basic integration time is 1 second and the scan duration is usually 60 seconds. The radiometric correction works then on timescales of a few seconds to one minute. It corrects only the amplitude: the phase is never changed because phase jumps between individual scans are dominated by instrumental limitations (mainly the receiver stability on a few minutes + ground pickup variations). The implications on the image quality are developed in Chapter 18. Longer atmospheric timescales of about $2-8$ hours are removed by the spline functions fitted inside the phase and the amplitude.

Intermediate timescales fluctuations from about one minute (the scan duration) to 1 hour are not removed. The resulting rms phase are measured by the fit of the splines in the phase. These timescales are not suppressed by the radiometric correction, and they contribute to the decorrelation factor f (see Eq.12.16), as the main component.

The decomposition of the atmospheric timescales for the PdBI observing method is given in table 12.3.

The method The differences in water vapor content are measurable by monitoring the variations of the sky emissivity T_{sky}. A monitoring of the total power in front of each antenna will then lead to a monitoring of the phase fluctuations. At Bure, we monitor the total power M_{atm} with the 1.3 mm receivers. The variation of T_{sky}, ΔT_{sky} (equal to ΔT_{emi}) is linked to the total power by

$$\frac{\Delta M_{atm}}{M_{atm}} = \frac{(\Delta T_{emi} + \Delta T_{loss})}{T_{sys}} \tag{12.18}$$

The monitoring of the atmospheric phase fluctuation works only when ΔT_{loss} due to the instrumentation is negligible on the timescales at which the phase correction is calculated and applied (typically a few seconds to one minute). Slow drifts on scale of hours have no effects.

With standard atmospheric conditions and following [Thompson et al. 1986] (their Eq.13.20), the variation of the path length through the atmosphere at zenith can be approximated by:

$$\Delta L = 6.3\delta w \tag{12.19}$$

were δw is the variation of water vapor content. ΔL is related to the phase fluctuation ψ_i above the antenna i by

$$\psi_i(t) = \frac{2\pi}{\lambda}\Delta L(t) \tag{12.20}$$

For example, under standard conditions (see fig.12.1 or 12.2), a variation $\delta w = 0.1$ mm corresponds to $\Delta L \simeq 630$ μm, $\Delta T_{sky} \simeq 1.5$ K and $\psi_i \simeq 250^o$ at 1.3 mm. This value is enormous and would not allow to produce images of good quality.

To reduce the phase fluctuation to a reasonable value having a negligible impact on the image quality *e.g.* $\psi_i \sim 25^o$, one needs to get $\Delta T_{loss} + \Delta T_{sky} \sim 0.15$ K corresponding to a global path length variation of $\sim 60\mu m$. For a typical $T_{sys} \sim 150$ K (DSB in the antenna plane, not SSB outside the atmosphere as for astronomical use), the instrumental stability required ($\Delta T_{loss}/T_{sys}$) must then be of order of $\sim 5 \cdot 10^{-4}$.

At Bure, on timescales of a few minutes, ΔT_{loss} is dominated by the stability of the receivers which must be carefully tuned to get the best stability. The 1.3 mm receivers are systematically tuned to get a stability of a few 10^{-4}; the stability is checked by doing autocorrelations of 60 seconds on the hot load. Achieving the required stability may prove impossible at some frequencies.

Practical implementation Ideally one would like to use T_{emi} measured each second on each antenna to compute $\psi_i(t)$ and correct the measured baseline phases. Practically, it is not so simple because $\psi_i(t)$ can do many turns and instrumental effects affect the measured T_{emi}.

Instead we use a differential procedure: once the antenna tracks a given source, one calibrates the atmosphere to calculate $T_{sys}(t_0)$, $\Delta L(t_0)$ and $\Delta L/dT_{sky}(t_0)$. Phase corrections are then referenced to t_0.

$$\Delta\psi_i = \frac{2\pi}{\lambda}\frac{d\Delta L}{dT_{emi}}\frac{T_{sys}(t_0)}{M_{atm}(t_0)}(M_{atm}(t) - M_{atm}(\mathrm{Ref})) \tag{12.21}$$

where $M_{atm}(\mathrm{Ref})$ is chosen in order to minimize as much as possible all the slow effects contributing to ΔT_{loss}. A long term atmospheric effect can also be included in $M_{atm}(\mathrm{Ref})$ because these effects are not removed by the radiometric phase correction but by the traditional phase referencing on a nearby calibrator. The main steps are the following:

1. The total power M_{atm} is continuously monitored on calibrators and on sources (every second).
2. Using the standard calibration method (see first part of the lecture) M_{atm} and T_{emi} (measured each second) are used to compute T_{sky} and w.
3. The atmospheric model has also been upgraded to compute the path length ΔL and its derivative $d\Delta L/dT_{emi}$. ΔL is computed by integrating the refractive index of the wet air along the line of sight across the atmosphere.
4. Within the 60 seconds scan, the new phase (Eq.12.21) is computed and the correction applied to the amplitude.

Quasi-real Time Calibration For the quasi-real time correction,

- the default value for $M_{atm}(\mathrm{Ref})$ is the measured atmospheric emission at the time of the last calibration, i.e. $M_{atm}(\mathrm{Ref}) = M_{atm}(t_0)$.

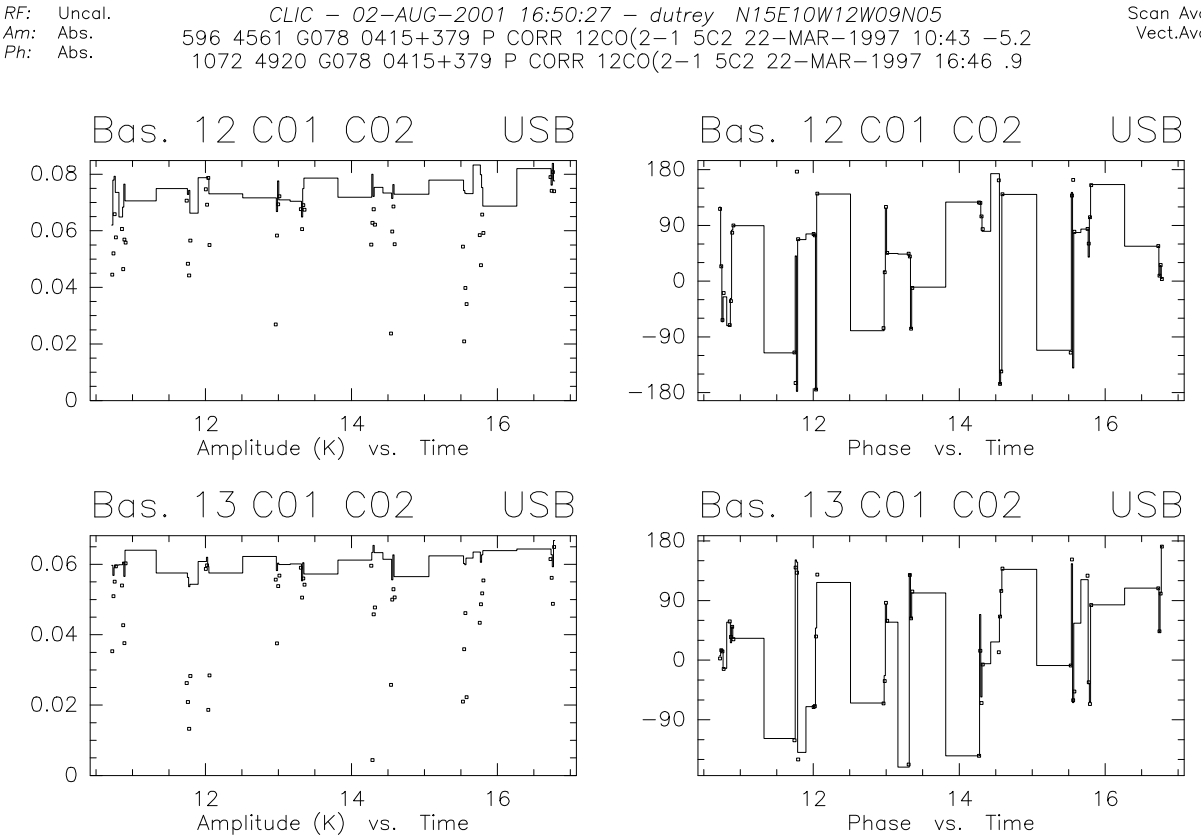

Figure 12.5: The amplitude and phase versus time on baselines B12 and B13 with (histogram) and without (points) the radiometric phase correction. The phase remains unchanged but the amplitude is significantly improved.

Calibrating using CLIC The CLIC command "**MONITOR** [*delta – time*]" allows to re-compute all the parameters. This command is useful when you want to select a better value for M_{atm}(Ref).

- This command is used to prepare the atmospheric radiometric phase correction. It processes the calibration scans to compute the correction factors (i.e. the change of path length for a given change in emission temperature of the atmosphere at the atmospheric monitor frequency (normally 1.3 mm)).

- The scans in the current index are grouped in intervals of maximum duration [*delta – time*] (in seconds); source changes will also be used to separate intervals. In each interval a straight line is fitted in the variation of atmospheric emission as a function of time; this line will be the reference value for the atmospheric correction, i.e. the correction at time t is proportional to the difference between the atmospheric emission at time t and the reference at time t. This scheme is used to avoid contaminating the correction with total power drifts of non-atmospheric origin (changes in receiver noise and gain, and changes in ground noise).

- `MONITOR 0` will use for each scan the average of the atmospheric emission as the reference value (i.e. $M_{atm}(\text{Ref}) =< M_{atm}(t) >_{scan}$). This will cause the correction to average to zero in one scan: the average phase is not changed, only the coherence is restored leading to an improved amplitude.

The automatic calibration procedure uses the command `MONITOR 0`.

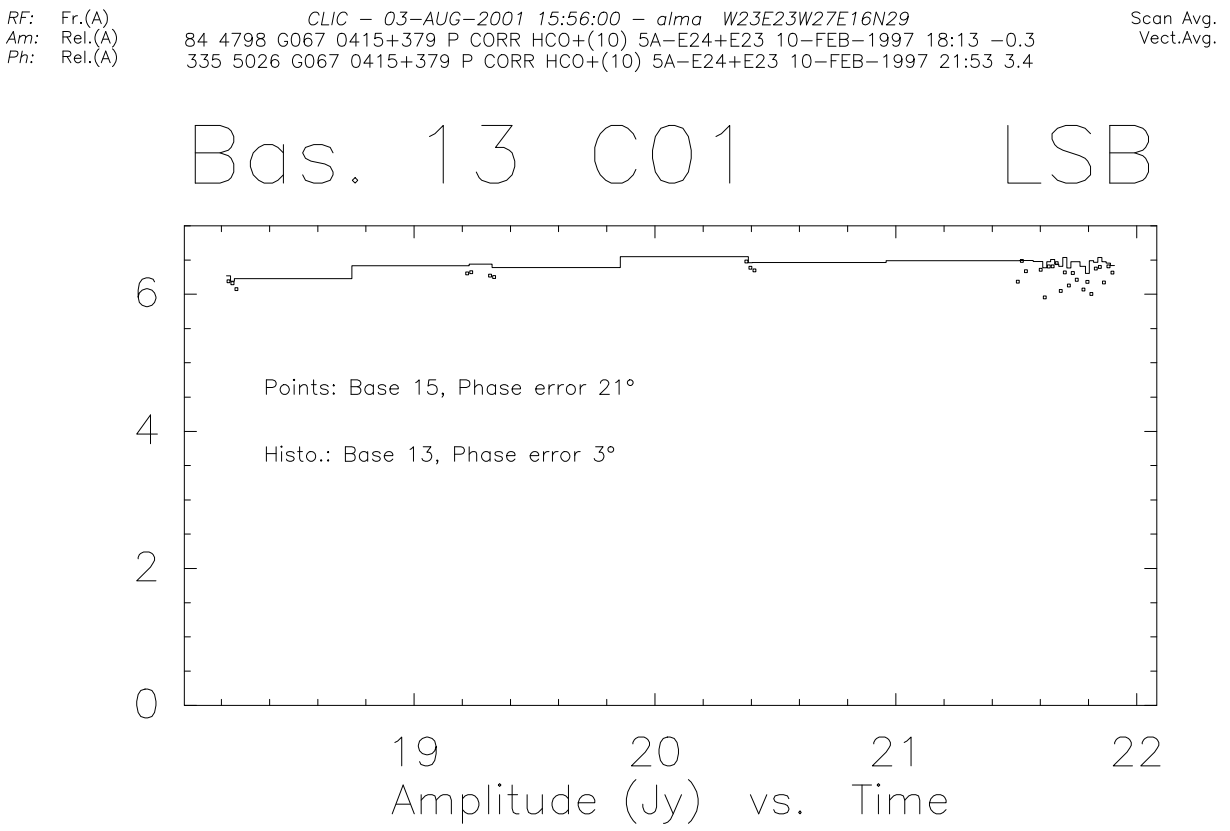

Figure 12.6: Example of calibrated amplitude (Jy) versus time on a short (B13) and a long (B15) baseline. The amplitudes are similar.

12.4.3 Fitting Splines: the last step

In the real-time processing, only the receiver gain and bandpass, the atmospheric transmission and the radiometric correction have been calibrated.

Fitting of the temporal variations of the global antenna gain (the so-called *amplitude calibration*) is performed in CLIC by fitting splines functions with time steps of 3-6 hours (`SOLVE AMPLITUDE [/WEIGHT] [/POL` *degree*`] [/BREAK` *time*`]`) and can be done either in baseline-based or in antenna-based mode. Note that in the latter case, the averaged amplitude closures are computed, as well as their standard deviations. The amplitude closures should be close to 100%. Strong deviations of amplitude closures from 100% are an indication of amplitude loss on long baselines, due to phase decorrelation during the time averaging. The fit then shows systematic errors; if this occurs, baseline based calibration of the amplitudes might be preferred.

The amplitude calibration involves interpolating the time variations of the antenna gains measured with the amplitude calibrator, assuming the its flux is known. The fitted splines must be as smoothed as possible in order to minimize the errors introduced on the source which is observed in between calibrators.

12.4.4 A few final checks

Once the amplitude calibration curve is stored, one can perform some simple checks on the calibrated data of the calibrator. These checks must be done in Jy (mode "`AMPLITUDE ABSOLUTE RELATIVE`" to the flux density of the calibrator).

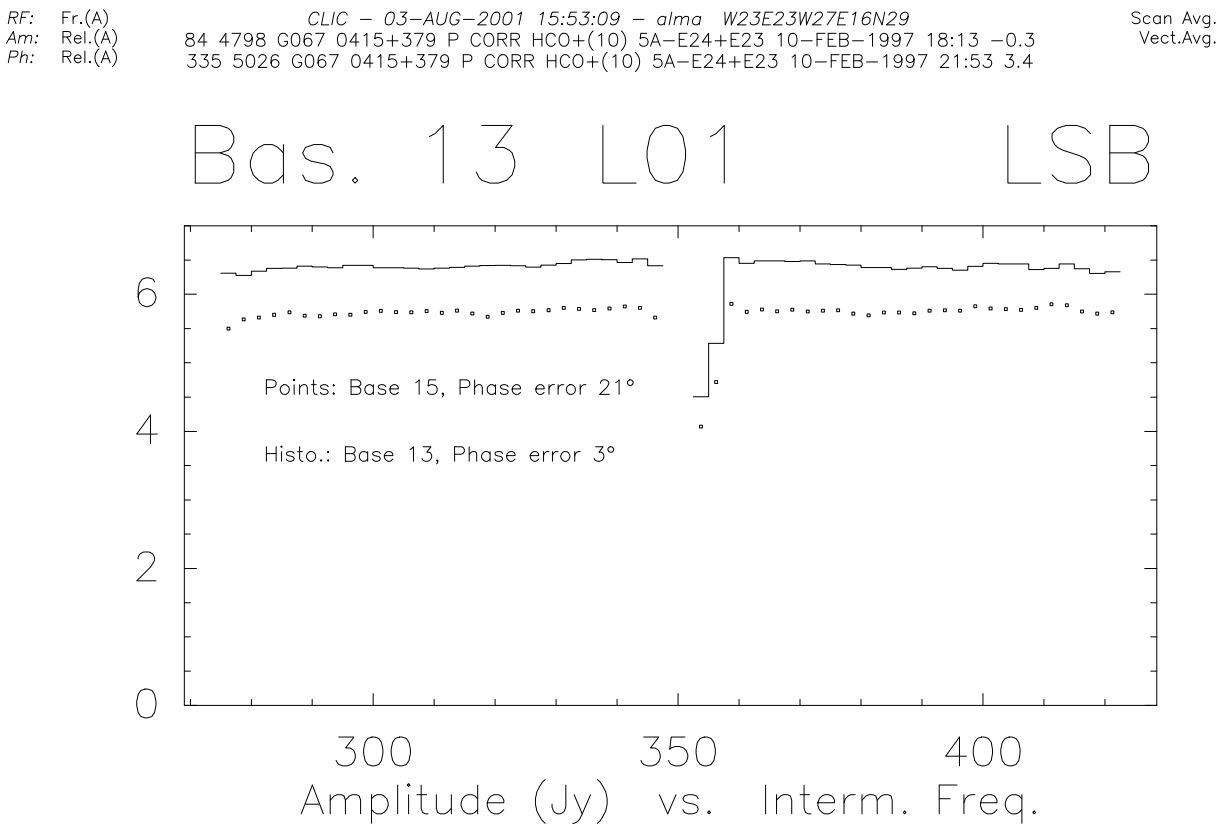

Figure 12.7: Example of calibrated amplitude versus IF frequency on a short (B13) and a long (B15) baseline. There is a significant loss of amplitude on the long baseline. The decorrelation factor is not calibrated out, and varies from short to long baselines. In this case, for the short baseline (B13), the decorrelation is completely negligible (see fig. 12.6).

Amplitude versus time On each baseline, the amplitude curves should be flat and equal to assume the flux density of the calibrator.

Amplitude versus IF frequency On each baseline, the amplitude curves should be flat, but they are not necessarily equal to flux of the calibrator because the decorrelation factor f is not taken into account here. To retrieve the flux density of the calibrator, they must be multiplied by the corresponding $e^{-(\Delta\phi)^2/2}$, where $\Delta\phi$ is baseline rms phase noise determined during the phase calibration.